Journal of Pharmacokinetics and Pharmacodynamics, Vol. 33, No. 5, October 2006 (© 2006)
DOI: 10.1007/s10928-006-9025-1

Semi-Mechanistic Pharmacodynamic Modeling for Degarelix, a Novel Gonadotropin Releasing Hormone (GnRH) Blocker*

Pravin R. Jadhav,[1,2] Henrik Agersø,[3] Christoffer W. Tornøe,[3] and Jogarao V.S. Gobburu[1,4]

Received March 20, 2006—Final June 5, 2006—Published Online August 8, 2006

An integrated semi-mechanistic pharmacodynamic (PD) model describing the relationship between luteinizing hormone (LH) and testosterone (T) after short-term administration of degarelix was developed. Data from three clinical studies involving, intravenous (IV) and subcutaneous (SC) dosing, in healthy male subjects were available. Degarelix pharmacokinetic (PK) data from all studies were modeled simultaneously. One intravenous study was used to develop the PD model and the two other studies (IV and SC dosing) were used to qualify the model. Degarelix PK follows a two-compartment model and exhibits flip-flop kinetics after subcutaneous dosing. Based on physiological mechanism, the gonadotropin releasing hormone (GnRH) time course was described using a pulsatile release model. A precursor-dependent pool model was used to describe the kinetics of LH in the pituitary and plasma compartment. In males, LH regulates T production in leydig cells. Degarelix inhibits the release of LH from the pool compartment to the plasma compartment leading to decreased T production. The plasma half-life of LH (2.6–3.3 hr) and T (2.7 hr) match well with the literature reports. The proposed PD model reasonably described the time course of LH and T including the LH rebound for short-term studies. The model predicted the time course of LH and T for the second IV and SC dosing studies very well. However, the long term simulations from the final model did not match with literature reports. A modification is suggested based on the physiological understanding of the system. The proposed novel modification to precursor models can be of general use for predicting long term responses.

KEY WORDS: hpg-axis; testosterone; GnRH; leutinizing hormone; pharmacokinetics; pharmacodynamics; degarelix.

*The views expressed in this article are those of the authors and do not necessarily reflect the official views of FDA.

[1]Pharmacometrics, Office of Clinical Pharmacology and Biopharmaceutics, Center for Drug Evaluation and Research, 10903 New Hampshire Avenue, Building 21, Silver Spring, MD 20993, USA.
[2]Department of Pharmaceutics, Medical College of Virginia, Virginia Commonwealth University, Richmond, VA 23298, USA.
[3]Experimental medicine, Ferring pharmaceuticals A/S, Copenhagen, Denmark.
[4]To whom correspondence should be addressed. e-mail: jogarao.gobburu@fda.hhs.gov

1567-567X/06/1000-0609/0 © 2006 Springer Science+Business Media, Inc.

INTRODUCTION

Prostate cancer is a major public health concern (1) accounting for 43% of new cancer cases among American men and second (14%) only to lung cancer (32%) as a cause of cancer related deaths. (2, 3) A variety of treatment options are available at different stages of the disease ranging from observation, prostatectomy, radiation and chemotherapy or hormonal therapy. Hormonal therapy offers a few alternatives ranging from estrogen, gonadotropin releasing hormone (GnRH) agonist and recently, GnRH blockers. (1)

For the last couple of decades, GnRH agonists, leuprolide, buserelin and goserelin, have been the standard of care during locally advanced stage of cancer as evidenced by world sales above 3.0 billion U.S. dollars in 2003. (4) However, GnRH agonists initially stimulate luteinizing hormone (LH) production causing testosterone (T) and dihydrotestosterone (DHT) surge for 5–12 days before inhibition by receptor desensitization. This surge can cause a flare reaction ('Clinical flare') and could be painful and often dangerous. (5) On the other hand, GnRH blockers suppress gonadotropin release from the pituitary gland leading to suppression of T levels and do not trigger a flare reaction. Therefore, GnRH blockers have been investigated for the management of prostate cancer and other sex-steroid dependent pathologies. Recently, the first GnRH blocker with prolonged effect, abarelix, was approved by the United States Food and Drug Administration for the palliative treatment of advanced symptomatic prostate cancer. (6) Degarelix, a GnRH blocker, is under clinical evaluation for the treatment of advanced prostate cancer. Degarelix has been shown to produce rapid and long-lasting suppression of the hypothalamic–pituitary–gonadal (HPG) axis in rats and non-human primates compared to other drugs in its class (7).

A few reports attempting to explain pharmacodynamic (PD) effects of GnRH blockers are available. (8–12) In these reports, the effect of GnRH blockers on LH and T is analyzed independently. Due to interdependence of LH and T, such models do not represent the mechanistic understanding of the physiological system. Therefore, a model integrating complex interaction within the HPG axis would offer insights about the physiology of control of LH and T. A mechanistic pharmacostatistical, pharmacokinetic-pharmacodynamic (PKPD), model is useful in (i) understanding and describing the physiological system (13, 14) (ii) simulating several *what-if* scenarios that are practically impossible to test by experimentation and (iii) selecting drug doses and/or dosing regimens to be studied in future trials or for labeling purposes. A more rational PKPD based drug development is particularly suited in developing GnRH blockers for several

reasons. First, empirical testing would be costly due to longer trials and challenges in recruiting patients. Second, the endpoint used for regulatory approval expects more than the conventional *P*-value. To demonstrate effectiveness, it is expected to have about 90% patients with T level below 0.5 ng/ml. Finally, a great deal of prior information from similar drugs is readily available to derive expectations at various stages of development.

The objectives of the current work were to (1) Develop an integrated mechanistic PKPD model describing the relationship between GnRH, LH and T after short-term IV administration of degarelix. (2) Evaluate the PKPD model by comparing the predictions to the observed data collected in two other studies with IV and SC administration. (3) Predict effects on T upon long-term administration of degarelix using simulations.

MATERIAL AND METHODS

Study Designs

For the current analysis, data from 3 short-term clinical trials were available. In Studies 1 and 2, healthy men received intravenous (IV) doses of degarelix, while in Study 3 degarelix was administered subcutaneously (SC). One of the principal aims of these early clinical trials is to select a rational dose and regimen for the long-term studies. All three studies were included in estimating the PK parameters. Study 1 was used to develop a PD model and other two studies were used to qualify the model.

Study 1: This was a single center, randomized, placebo-controlled, single-dose, constant-infusion study with parallel IV treatment groups. A total of 48 healthy male subjects aged at least 65 years with normal serum T levels and normal creatinine clearance were randomized to seven treatment groups (groups A to G). The subjects were admitted to the clinic the day before dosing and followed for 72 hr after dosing. The dosing scheme is given in Table I.

Blood samples for quantifying degarelix, LH and T were collected at the following times: pre-dose, 30 min, 1, 2, 4, 6, 8, 10, 12, 15, 18, 24, 36, 48, 60, 72, 96 hr after start of infusion.

Study 2: This was a single center, randomized, single-dose, IV infusion study. A total of 24 healthy male subjects with normal serum T levels and normal creatinine clearance were randomized to four treatment groups (groups I – IV). The subjects were admitted to the clinic the day before dosing and followed for 14 days after dosing. The dosing scheme is given in Table I.

Blood samples for quantifying degarelix, LH and T were collected at the following times: pre-dose, during infusion a number of times (see below), at 5, 10, 15, 30, 45 min, 1, 2, 4, 8, 12, 24, 36, 48 hr, and on days 3,

Table I. Dosing Regimen for Study 1, 2 and 3

Group	*N*	0–1hr (μg/kg)/h	1–6hr (μg/kg)/hr	6–48hr (μg/kg)/h	Total dose μg/kg
Study 1					
A	6	0	0	0	0
B	6	0.0887	0.0257	0.0154	0.864
C	6	0.177	0.0514	0.0308	1.73
D	6	0.38	0.11	0.066	3.7
E	6	1.01	0.294	0.176	9.87
F	9	2.53	0.734	0.44	24.7
G	9	5.07	1.47	0.88	49.4
Study 2					
I	6	6	15 min infusion		1.5
II	6	25			6
III	6	20	45 min infusion		15
IV	6	40			30
Study 3		Dosing solution conc. (mg/ml)			Total dose mg
1	6	5			0.5
2	6	5			2
3	6	10			5
4	6	10			10
5	6	10			20
6	6	20			40
7	6	10			40
8	6	20			40
9	6	15			30
10	6	30			30
11	20	0			0

4, 7 and 10 after infusion. For subjects receiving 15 min infusion or 45 min infusion, blood samples were drawn at 5, 10 min and 15, 30 min, respectively, during infusion.

Study 3: This was a single center, randomized, placebo-controlled single SC dose escalation study. A total of 80 healthy male subjects with normal serum T levels and normal creatinine clearance were randomized to eleven treatment groups (groups 1–11). The following dose levels were included in the study: placebo, 0.5, 2, 5, 10, 30, and 40 mg/subject at concentrations ranging from 5 to 30 mg/ml in the dosing solution. The dosing scheme is given in Table I.

Blood samples for quantifying degarelix, LH and T were collected at the following times: pre-dose and 5, 15, 30, 45 min, 1, 1.5, 2, 4, 6, 8, 12, 24 hr, and on days 2, 4, 9, 13, 20, 29, 36, 43, 51 and 59 after dosing.

Analytic Methods

Degarelix concentrations were measured by liquid chromatography using tandem mass spectrometric detection (LC-MS/MS) with lower limit of quantification (LLOQ) of 0.5 ng/ml. The intra- and inter-assay precision were less than or equal to 7.5% and 14.1%, respectively. The accuracy was within ±3%. The LH assay was based on the Microparticle Enzyme Immunoassay (MEIA) technology (Abbott Laboratories, IL) with an LLOQ of 0.1 IU/l. The intra- and inter-assay precision were less than or equal to 5.7% and 5.3%, respectively. The accuracy was within ±11%. Total serum T concentrations were measured according to LC-MS/MS after solid phase extraction with an LLOQ of 0.05 ng/ml. The intra- and inter-assay precision were less than or equal to 15.8% and 14.1%, respectively. The accuracy was within ±8%.

Model Building

Pharmacokinetic Model

Degarelix PK data from all three studies were modeled simultaneously with a previously reported population PK model shown in Fig. 1. (14) Degarelix follows a two compartment body model after IV administration. The model assumes that degarelix given SC was absorbed by a slow ($k_{a,slow}$) and a fast ($k_{a,fast}$) first order process. The following set of ordinary differential equations was used to describe the PK model.

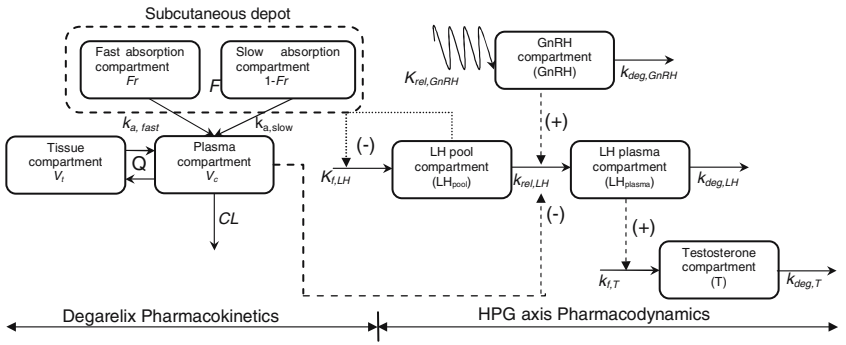

Fig. 1. Schematic PKPD model for degarelix, GnRH, LH and T concentration. Solid lines (——) indicate compartmental transfer of biomaterial, broken lines (- - - - -) indicate feedforward interaction, dotted lines (·····) indicate feedback interaction. A positive sign (+) indicates stimulatory control and a negative sign (−) indicates inhibitory control.

$$\frac{dX_{\text{sc,fast}}}{dt} = -k_{\text{a,fast}} \cdot X_{\text{sc.fast}} \tag{1}$$

$$\frac{dX_{\text{sc,slow}}}{dt} = -k_{\text{a,slow}}^{\text{conc}} \cdot X_{\text{sc.slow}} \tag{2}$$

$$\frac{dX_{\text{c}}}{dt} = k_{\text{a,fast}} \cdot X_{\text{sc.fast}} + k_{\text{a,slow}}^{\text{conc}} \cdot X_{\text{sc.slow}} + Q \cdot \left(\frac{X_{\text{t}}}{V_{\text{t}}} - \frac{X_{\text{c}}}{V_{\text{c}}}\right) - CL \cdot \frac{X_{\text{c}}}{V_{\text{c}}} \tag{3}$$

$$\frac{dX_{\text{t}}}{dt} = Q \cdot \left(\frac{X_{\text{t}}}{V_{\text{t}}} - \frac{X_{\text{c}}}{V_{\text{c}}}\right) \tag{4}$$

where $X_{\text{sc,fast}}$, $X_{\text{sc,slow}}$, X_{c} and X_{t} represent the amount of degarelix in the fast and slow SC depot compartments, plasma (central) and tissue (peripheral) compartments, respectively. CL, Q, V_{c} and V_{t} represent clearance from the plasma compartment, intercompartmental clearance, volume of the plasma compartment and volume of the tissue compartments, respectively. The SC dose was partitioned into fast [$\text{Fr}^{\text{conc}}.\text{F}^{\text{conc}}.\text{DOSE}_{\text{sc}}$] and slow [$(1 - \text{Fr}^{\text{conc}}) \cdot \text{F}^{\text{conc}} \cdot \text{DOSE}_{\text{sc}}$] absorption compartments, where, Fr, F and DOSE_{sc} refers to the fraction of the administered dose for the fast absorption process, the absolute bioavailability and the input from the SC degarelix dose at time of administration, respectively. The parameters F, Fr and $k_{\text{a,slow}}$, were allowed to vary with different dosing solution concentration.

The first-order absorption rate constant $k_{\text{a,fast}}$ associated with the fast absorption components was estimated as the absorption half-life $t_{1/2,\text{fast}}$. To ensure that the slow absorption half-life $t_{1/2,\text{slow}}$ was constrained to be larger than $t_{1/2,\text{fast}}$ even after taking inter-individual variability (IIV) into account, the following parameterization was chosen.

$$t_{1/2,\text{slow,i}} = t_{1/2,\text{slow}-\text{fast}} \cdot \exp\left(\eta_{t_{1/2,\text{slow}-\text{fast,i}}}\right) + t_{1/2,\text{fast,i}} \tag{5}$$

where $t_{1/2,\text{slow}-\text{fast}}$ is the typical individual's difference between $t_{1/2,\text{fast}}$ and $t_{1/2,\text{slow}}$. The fraction of the dose absorbed via the fast absorption route (Fr) and the absolute bioavailability (F) parameters were constrained between 0 and 1 by logit transformation using Eqs. 6 and 7.

$$\rho = \log \frac{\text{Fr}}{1 - \text{Fr}} \tag{6}$$

$$\text{Fr} = \frac{\exp(\rho)}{1 - \exp(\rho)} \tag{7}$$

The IIV for $t_{1/2,\text{fast}}$, $t_{1/2,\text{slow}}$, CL and V_{c} was assumed to follow a log-normal distribution which was described using an exponential error model.

The residual error was assumed to follow a combined additive and proportional error model. The goodness of fit was assessed by plotting population and individual predictions versus observed data, inspecting representative individual time–concentration profiles and comparing PK parameter estimates with the previously reported values.

Pharmacodynamic Model

Study 1 data were used for building the PD model. The population mean concentrations were used to drive the PD model. Several attempts, including fixing some parameters to reported literature estimates, were made to develop a mixed effect model for the PD analyses. Because numerical solution to the complex differential equations used here must be obtained, the initial attempts showed that the fitting could result in long computational time and model convergence problems. Therefore, a mixed effects model for the PD analyses was not used. More importantly, the IIV of the maximal response was ~40%. Hence modeling group means was considered reasonable.

Figure 1 provides a schematic representation of the processes involved in the HPG axis. It has been shown that the hormonal regulation at the HPG axis is a complicated multivariate closed loop system with several feedback and feedforward interactions. (14) GnRH is formed in the preoptic area of the hypothalamus; it is transported via the hypothalamic-hypophyseal portal microcirculatory system, to the anterior pituitary gland. GnRH is secreted in a pulsatile manner that governs the synthesis and pulsatile release of the gonandotropins, LH and follicle stimulating hormone (FSH). (15) Using animal models, it has been shown that GnRH is a major factor governing the LH pulses and there is a one-to-one relation between GnRH and LH pulses. (16–18) These pulses follow an ultradian rhythm with approximately one event every 60–120 min. (19) The time course of GnRH was described using Eq. 8.

$$\frac{d\mathrm{GnRH}}{dt} = K_{\mathrm{rel,GnRH}} - k_{\mathrm{deg,GnRH}} \cdot \mathrm{GnRH} \tag{8}$$

where $K_{\mathrm{rel,GnRH}}$ is the zero order pulse rate at a frequency of 2 hr and $k_{\mathrm{deg,GnRH}}$ is the first order degradation rate constant for GnRH.

A GnRH blocker inhibits LH release to elicit therapeutic benefit. Eqs. 9 and 10 describe the kinetics of LH in the pool and plasma compartments.

$$\frac{d\mathrm{LH}_{\mathrm{pool}}}{dt} = K_{\mathrm{f,LH}} - k_{\mathrm{rel,LH}} \cdot \mathrm{GnRH} \cdot \mathrm{LH}_{\mathrm{pool}} \cdot I(C) \tag{9}$$

$$\frac{d\mathrm{LH}_{\mathrm{plasma}}}{dt} = k_{\mathrm{rel,LH}} \cdot \mathrm{GnRH} \cdot \mathrm{LH}_{\mathrm{pool}} \cdot I(C) - k_{\mathrm{deg,LH}} \cdot \mathrm{LH}_{\mathrm{plasma}} \tag{10}$$

where $K_{\mathrm{f,LH}}$ is the zero order formation rate constants for LH, $k_{\mathrm{rel,LH}}$ is the rate constant governing the release of LH to the plasma compartment, $k_{\mathrm{deg,LH}}$ is the first order degradation rate constant for LH and $I(C)$ is the inhibitory effect of degarelix on the release of LH from the pool compartment given by Eq. 11.

$$I(C) = 1 - \frac{C}{IC_{50} + C} \tag{11}$$

where C is the degarelix plasma concentration and IC_{50} is the degarelix plasma concentration which produces 50% of maximum inhibition of $k_{\mathrm{rel,LH}}$. Preliminary graphical inspection indicated that degarelix is capable of completely suppressing LH release. Hence the maximal suppression was fixed at 100% (i.e. $I_{\max} = 1$).

In males, LH regulates T production in testicular leydig cells by interacting with the LH receptors. Testosterone is primarily responsible for normal growth and development of male sex and reproductive organs as well as secondary male characteristics. A clear temporal correlation between LH and T pulses has been shown (20). Equation 12 illustrates the kinetics of T regulation by plasma LH levels.

$$\frac{dT}{dt} = k_{\mathrm{f,T}} \cdot \mathrm{LH}_{\mathrm{plasma}} - k_{\mathrm{deg,T}} \cdot \mathrm{T} \tag{12}$$

where $k_{\mathrm{f,T}}$ is the formation rate constant for T and $k_{\mathrm{deg,T}}$ is the first order degradation rate constant for T.

All the compartments (GnRH, $\mathrm{LH}_{\mathrm{pool}}$, $\mathrm{LH}_{\mathrm{plasma}}$, T) in the system were assumed to be at steady state before drug administration. The following equations describe steady state levels for each compartment.

$$\mathrm{GnRH}_0 = \frac{1}{1 - e^{-k_{\mathrm{deg,GnRH}} \cdot \tau}} e^{-k_{\mathrm{deg,GnRH}} \cdot \tau} \tag{13}$$

$$\mathrm{LH}_{\mathrm{pool}_0} = \frac{K_{\mathrm{f,LH}}}{k_{\mathrm{rel,LH}} \cdot \mathrm{GnRH}_0} \tag{14}$$

$$\mathrm{LH}_{\mathrm{plasma}_0} = \frac{k_{\mathrm{rel,LH}} \cdot \mathrm{GnRH}_0 \cdot \mathrm{LH}_{\mathrm{pool}_0}}{k_{\mathrm{deg,LH}}} \tag{15}$$

$$T_0 = \frac{k_{\mathrm{f,T}} \cdot \mathrm{LH}_{\mathrm{plasma}_0}}{k_{\mathrm{deg,T}}} \tag{16}$$

where $GnRH_0$, LH_{pool_0}, LH_{plasma_0} and T_0 are the baseline states of GnRH, LH_{pool}, LH_{plasma} and T compartments before drug administration and τ is the GnRH pulse frequency of 2 hr. The following parameters, $K_{f,LH}$, $k_{rel,LH}$, $k_{deg,LH}$, $k_{f,T}$, $k_{deg,T}$, IC_{50}, were estimated and the above baseline estimates were derived from these fitted parameters. The goodness of fit was assessed by plotting observed and predicted time course for each dose group and, more importantly, comparing the parameter estimates with the values available in literature.

Model Qualification

Studies 2 and 3 were used to assess the predictive ability of the model. The model developed using Study 1 (IV) was employed to predict the mean time course of LH and T, according to the design of the Studies 2 (IV) and 3 (SC). The population mean degarelix concentrations from studies 2 and 3 were used for the PD simulations.

The final model was also used to predict the time course of LH and T after long term administration of degarelix. A typical individual was assumed to be given 40 mg SC dose (20 mg/ml degarelix in the dosing solution) once a week for 6 weeks.

Data Analysis

Sequential PKPD modeling was performed using NONMEM version V with Compaq digital Fortran compiler on DELL Latitude Intel P4 with 1.8 GHz processor and 512 MB RAM running Windows XP professional. The population PK predictions were used to drive the PD model. The first-order conditional estimation (FOCE) method was used throughout the PKPD model development using the subroutine ADVAN5 TRANS1 for the PK analysis and ADVAN9 for the PD analysis. Data from all doses were modeled simultaneously.

RESULTS

Model Building

Pharmacokinetics

A total of 126 subjects were included in the PK modeling. Degarelix plasma concentrations displayed a biphasic disposition. Representative observed and predicted degarelix concentration-time profiles for the IV and SC studies are shown in Fig. 2. The SC profiles (Panels c and d)

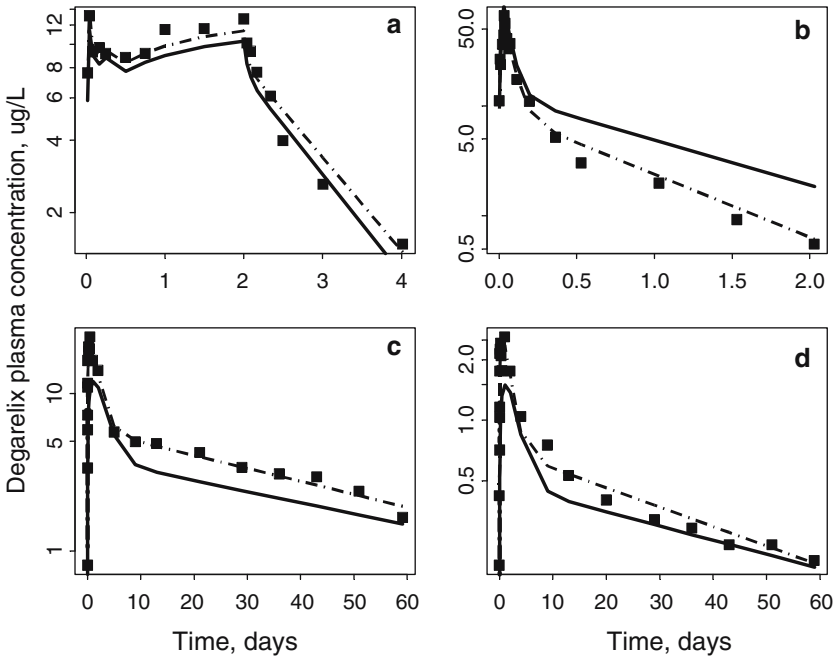

Fig. 2. Representative individual plots from a (Study 1: 24.7 μg/kg), b (Study 2: 15 μg/kg), c and d (Study 3: 40 mg and 5 mg at 10 mg/ml). Observed degarelix plasma concentration (symbols), population predictions (solid line) and individual predictions (dotted line) are presented.

show a prolonged terminal phase, with concentrations detectable until 60 days after single dose administration. Comparison of the disposition phases for the IV (Panels a and b) and SC data indicates flip-flop kinetics, i.e., slower absorption relative to the elimination. The basic goodness of fit plots of individual and population predictions vs. observed concentrations are shown in Fig. 3. The scatter of data points around the line of identity indicates good agreement between the model predictions and observed data. The model predicted degarelix concentration–time profile to differentiate between dose groups is presented in Fig. 4. For simplicity, only three dose groups (low, medium, high) for study 3 are included.

The population PK parameter estimates are reported in Table II. The population mean CL was 2.91 l/hr and the population mean V_c was 11.4 l. For the SC dosing, $t_{1/2,\text{fast}}$ was 1.17 day and the $t_{1/2,\text{slow}}$ increases with increasing dosing solution concentration. The $t_{1/2,\text{slow}}$ estimate ranged between 41.5 days for the 5 mg/ml dosing solution to 70.3 for the 30 mg/ml dosing solution. The absolute bioavailability, F, decreases with increasing

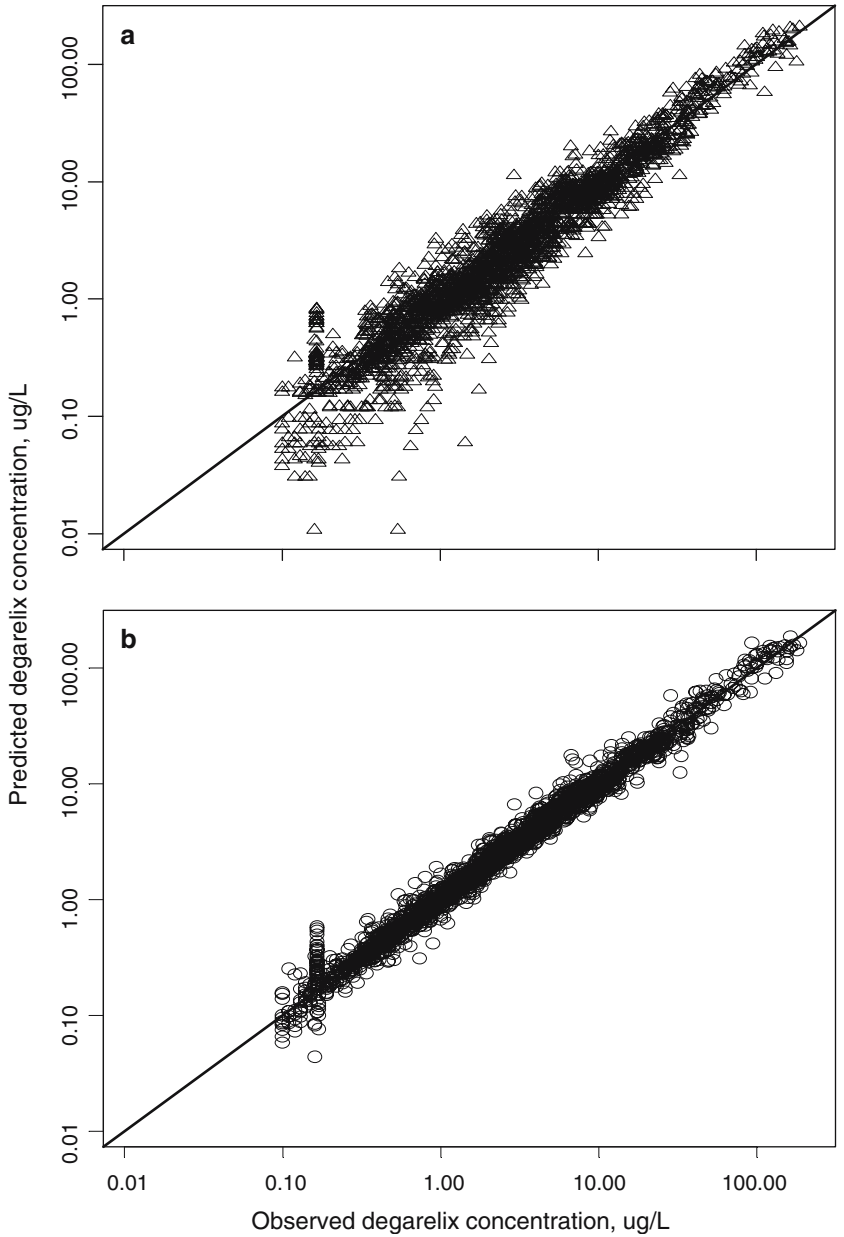

Fig. 3. Plot of (a) population predictions (triangles) and (b) individual (circles) predictions vs. observed degarelix concentrations from the IV and SC studies. The solid line indicates the line of identity.

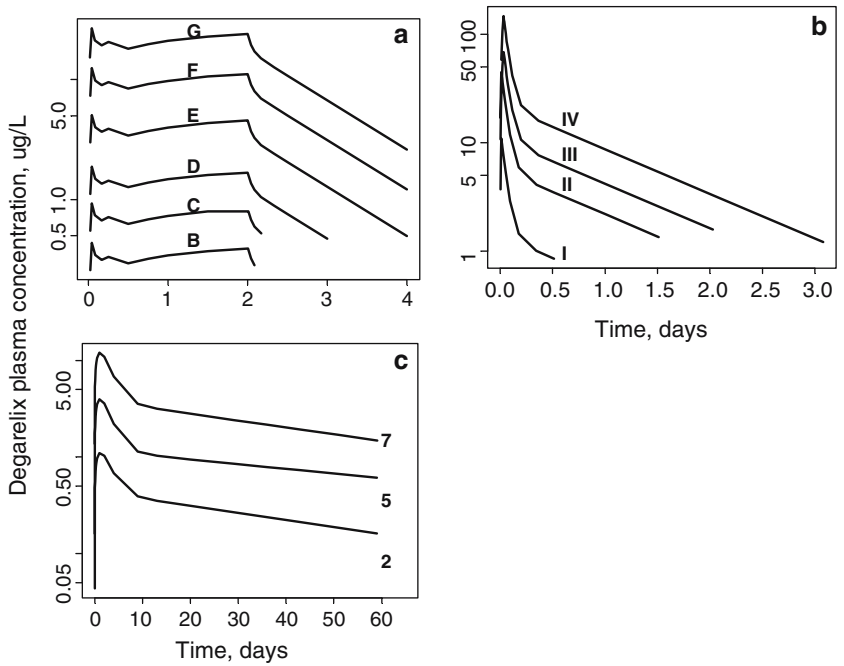

Fig. 4. Plot of population predicted degarelix concentration vs. time for (a) all study 1 groups (b) all study 2 groups and (c) three study 3 groups.

dosing solution concentration. The range of F was estimated to be 100% for the 5 mg/ml dosing solution to 34% for the 30 mg/ml dosing solution. The fraction of the dose absorbed via the fast absorption route (Fr) was relatively small, ranging between 8.5% and 14%. The IIV on all the parameters, as expressed by %CV, was small. The IIV on Q, V_t and F could not be estimated and was fixed to zero.

Pharmacodynamics

The PD model predictions for LH and T levels from Study 1 are shown in Figs. 5 and 6. The LH levels reach nadir in about 0.5 day and as degarelix concentrations fall below the IC_{50}, LH levels gradually reach baseline with a rebound effect in about 2 days. Although, the baseline LH and T levels are highly variable, the variability in PD effect is noticeably low. Degarelix lowers the LH and T levels in a concentration-dependent manner. The duration of drug action also exhibits dose-dependency with slower recovery phase with increasing degarelix doses. The rebound phenomenon is apparent in LH time profiles for almost all the groups. The

Table II. Summary of Population PK Estimates for Degarelix Following IV and SC Administration

Parameter	Units	Population estimate	IIV (% CV)	Definition
CL	l/hr	2.91	26.6	Clearance
V_c	l	11.40	55.7	Volume of distribution in the plasma compartment
Q	l/hr	6.04	NE	Intercompartmental clearance
V_t	l	44.30	NE	Volume of distribution in the tissue compartment
$t_{1/2,\text{fast}}$	day	1.17	57.8	Absorption half-life for the fast-absorption process
$t^{5}_{1/2,\text{slow}}$	day	41.50	21.9[a]	
$t^{10}_{1/2,\text{slow}}$	day	42.83	22.0[a]	Absorption half-life for the
$t^{15}_{1/2,\text{slow}}$	day	49.08	22.0[a]	slow-absorption process; the
$t^{20}_{1/2,\text{slow}}$	day	62.42	22.1[a]	superscript represents the
$t^{30}_{1/2,\text{slow}}$	day	70.33	22.1[a]	dosing solution concentration
F^5	–	1.00		
F^{10}	–	0.47		Absolute bioavailability; the
F^{15}	–	0.42	NE	superscript represents the
F^{20}	–	0.41		dosing solution concentration
F^{30}	–	0.34		
Fr^5	–	0.10	24.8[b]	Fraction of the administered
Fr^{10}	–	0.12	24.2[b]	dose for the fast absorption
Fr^{15}	–	0.14	23.7[b]	process; the superscript
Fr^{20}	–	0.10	24.9[b]	represents the dosing solution
Fr^{30}	–	0.09	25.2[b]	concentration

CV: Coefficient of variation; NE: Not estimated.

$t_{1/2,\text{slow}} = t_{1/2,\text{slow}-\text{fast}} + t_{1/2,\text{fast}}$.

[a] $\text{CV}\left(t^{\text{conc}}_{1/2,\text{slow}}\right) = \left(\left(t^{\text{conc}}_{1/2,\text{slow}-\text{fast}}\right)^2 \cdot \omega^2_{t^{\text{conc}}_{1/2,\text{slow}-\text{fast}}} + \left(t_{1/2,\text{fast}}\right)^2 \cdot \omega^2_{t_{1/2,\text{fast}}}\right)^{1/2} \Big/ \left(t_{1/2,\text{fast}} + t^{\text{conc}}_{1/2,\text{slow}-\text{fast}}\right)$

[b] $CV(\text{Fr}) = (1 - \text{Fr}) \cdot \omega_{\text{Fr}}$.

ω represents IIV on the parameter of interest.

$t^{*}_{1/2,\text{slow}}$, F^{*} and Fr^{*}—a superscript represents the dosing solution concentration.

proposed precursor dependent model captures it well. The proposed PD model reasonably captures the time course of LH and T after IV administration in Study 1. The population mean PD parameter estimates are reported in Table III. The plasma half-life of LH and T was found to be 2.6–3.3 and 2.7 hr, respectively. The estimate of IC_{50} was found to be 0.45 μg/l.

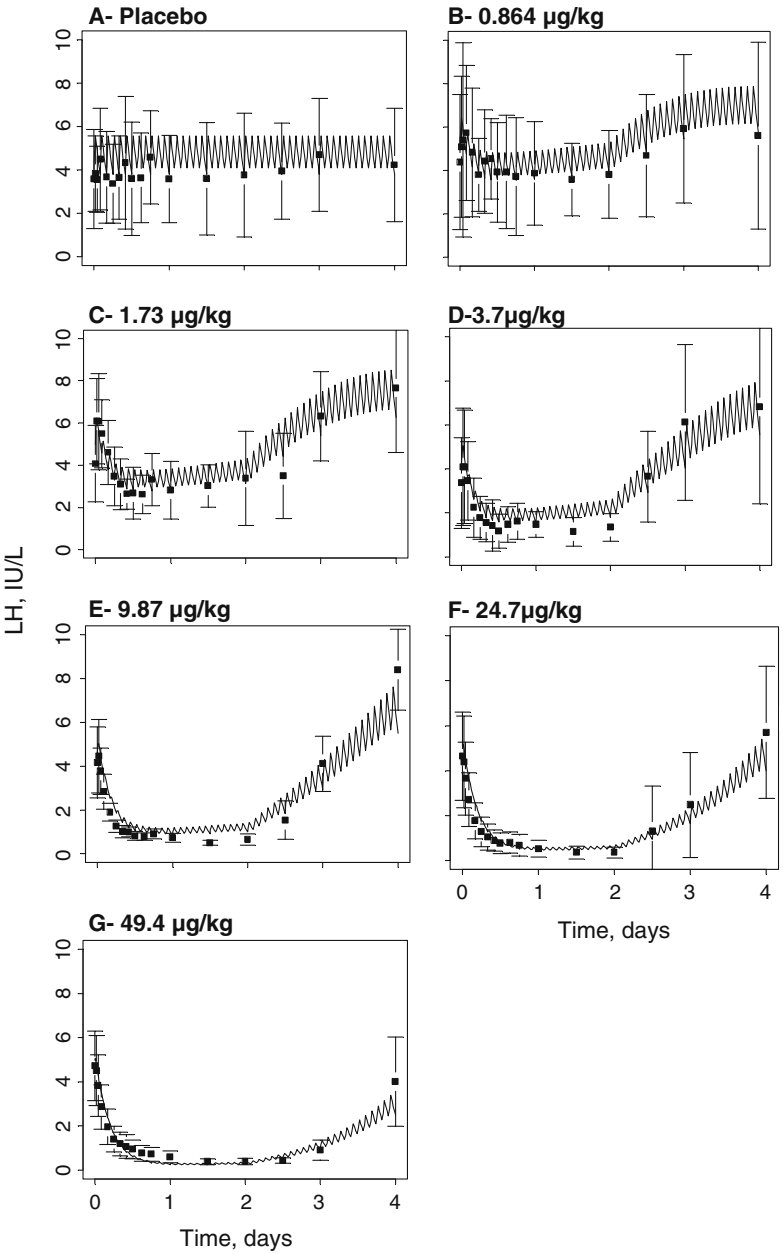

Fig. 5. The time course of observed mean (symbols) and predicted (solid line) LH levels from Study 1. The error bars correspond to one standard deviation.

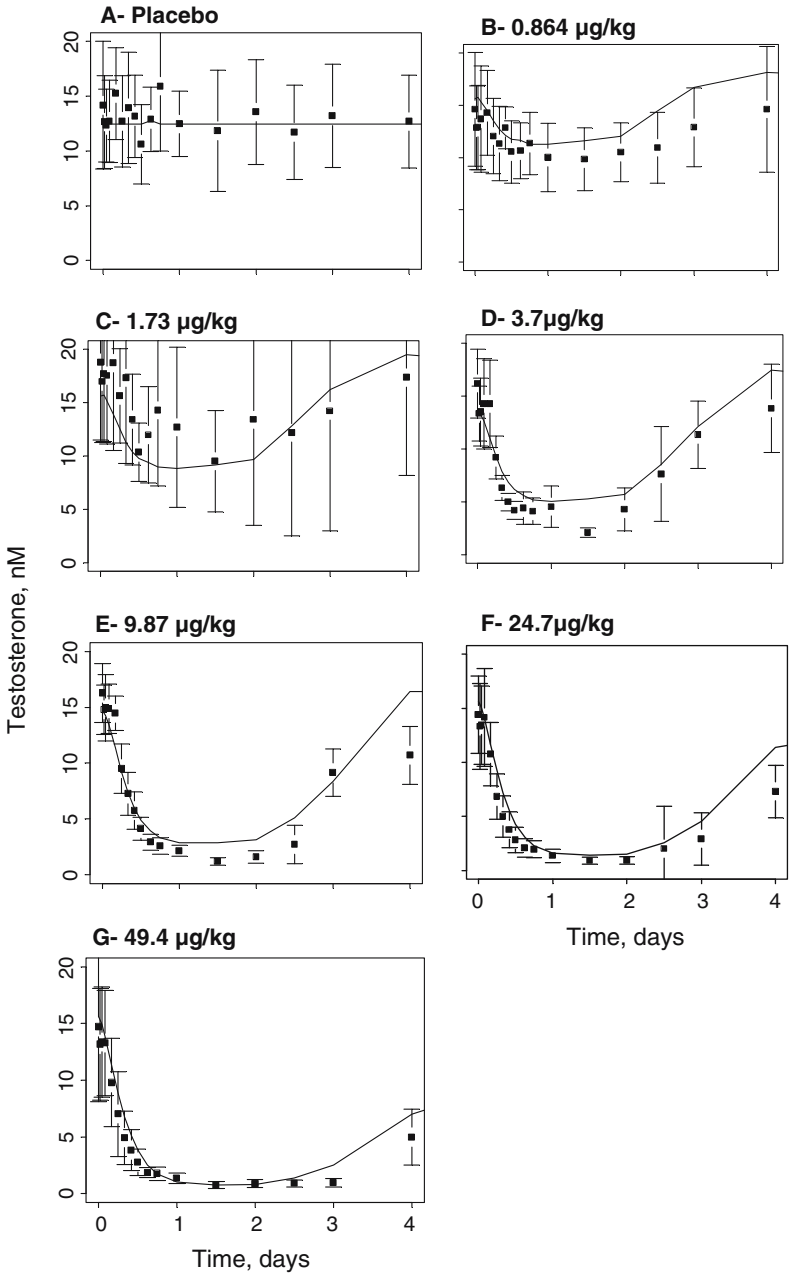

Fig. 6. The time course of observed mean (symbols) and predicted (solid line) T levels from Study 1. The error bars correspond to one standard deviation.

Table III. Summary of PD Estimates for Degarelix from Study 1

Parameter	Units	Estimate	Definition
$K_{f,LH}$	IU/l/hr	1.24	Formation rate of LH
$k_{rel,LH}$	l/IU/hr	0.63	Pulsatile release process for GnRH
$k_{deg,LH}$	per hr	0.21	
$k^{A}_{deg,LH}$	per hr	0.26	Degradation rate constant for LH
$k^{D}_{deg,LH}$	per hr	0.24	
$k^{E}_{deg,LH}$	per hr	0.22	
$k_{f,T}$	l/hr/IU	0.68	Formation rate constant for T
$k_{deg,T}$	per hr	0.26	Degradation rate constant for T
IC_{50}	μg/l	0.45	Degarelix plasma concentration which produces 50% of maximum inhibition of $k_{rel,LH}$

$k^{*}_{deg,LH}$—a superscript represents the group number for which the parameter was allowed to vary thus accounting for baseline differences.

Model Qualification

The PD model developed using Study 1 (IV) was employed to predict the mean time course of LH and T, according to the design of the Studies 2 (IV) and 3 (SC). The time course of LH for Studies 2 and 3 are shown in Figs. 7 and 9. The time course of T for Studies 2 and 3 are shown in Figs. 8 and 10. The baseline hormone level meaningfully varied between the studies (Baseline T range–Study 1: 14.2–18.8 nM, Study 2: 16.8–21.7 nM, and Study 3: 8.7–22.5 nM). Simulations were conducted to match the mean baseline for the observed data by scaling the predictions with the ratio of observed and predicted baseline. Importantly, the predictions were independent of the real data. The simulated and observed data are in close agreement with an exception of higher LH rebound seen in some groups in Study 2 (Fig. 7). The LH rebound in groups I, II and III in the observed data is considerably higher, almost two times above the baseline, compared to Study 1. The model developed from the IV data performs considerably well after the SC administration of degarelix in Study 3.

Subsequently, the time course of LH and T after the administration of once a week 40 mg SC dose (20 mg/ml degarelix in the dosing solution) were simulated. Figure 10 provides the time course of degarelix, LH and T in a typical individual. Expectedly, the LH and T levels are suppressed considerably after the first dose. The LH and T levels seem to return to baseline even after maintaining degarelix concentrations well above the IC_{50} value.

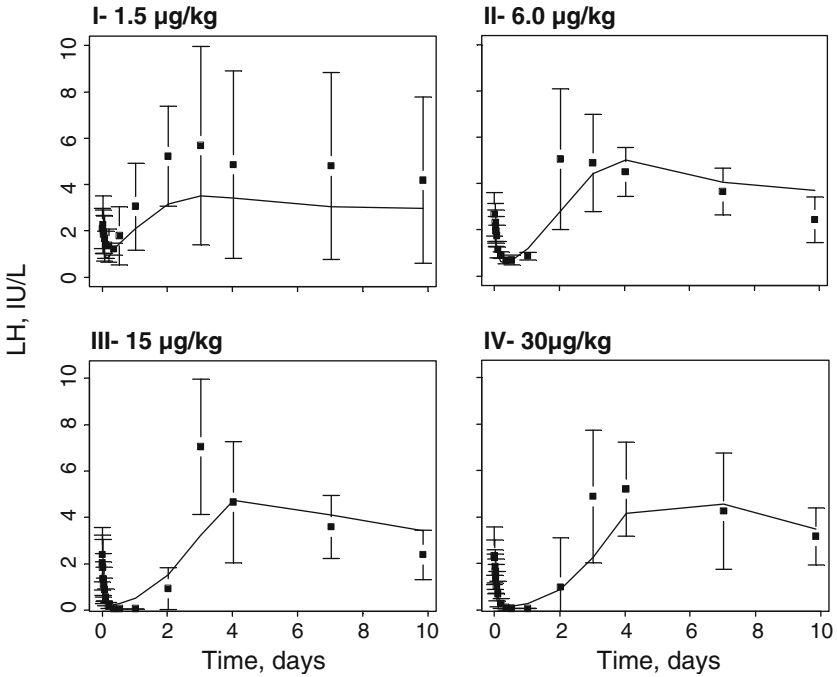

Fig. 7. The time course of observed mean (symbols) and simulated (solid line) LH levels from Study 2. The error bars correspond to one standard deviation.

DISCUSSION

Model Building

Pharmacokinetics

The assessment of individual time–concentration profiles and scatter of data points around the line of identity indicate that the proposed model describes degarelix PK reasonably well (Figs. 2 and 3). The estimated PK parameters are in close agreement with the previously reported estimates. (14) The SC administration of degarelix produced flip-flop PK behavior. It has been reported that an *in situ* depot formation is responsible for the prolonged degarelix release. The nature of the depot has not been well established, but interaction with the tissue proteins after SC or intramuscular (IM) administration is believed to form a gel like structure. (7, 21) This phenomenon results in a slow release of degarelix from the depot, resulting in detectable drug concentrations until 60 days after single dose administration. The formation of a depot is consistent with other

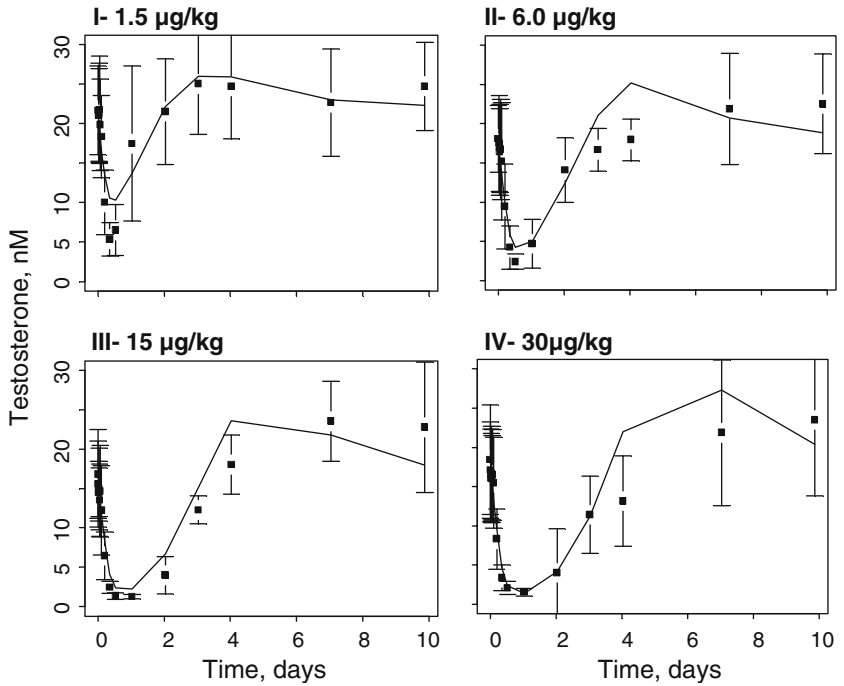

Fig. 8. The time course of observed mean (symbols) and simulated (solid line) T levels from Study 2. The error bars correspond to one standard deviation.

drugs, such as abarelix and cetrorelix, as evidenced by the prolonged terminal half-life after SC or IM administration. Degarelix exhibits longer terminal half-life (>40 days) compared to abarelix (~ 13 days) and cetrorelix (~ 2.5 days) (6, 8). The slow-release depot structure could be an advantage in the treatment of prostate cancer, because drug concentration can be maintained for longer period of time with a low dosing frequency.

Pharmacodynamics

The GnRH compartment (Eq. 1) model was based on the literature data. GnRH is responsible for the pulsatile pattern observed in LH and FSH levels. The pulse frequency, one pulse every 2 hr, was obtained from the literature (19). GnRH levels were not available, therefore, a unit dose for the duration of 0.1 hr was introduced and $k_{\text{deg,GnRH}}$ was fixed to $10\,\text{hr}^{-1}$ to obtain a pulse of one unit in magnitude. More complex biomathematical models are available (22). However, our aim was to obtain

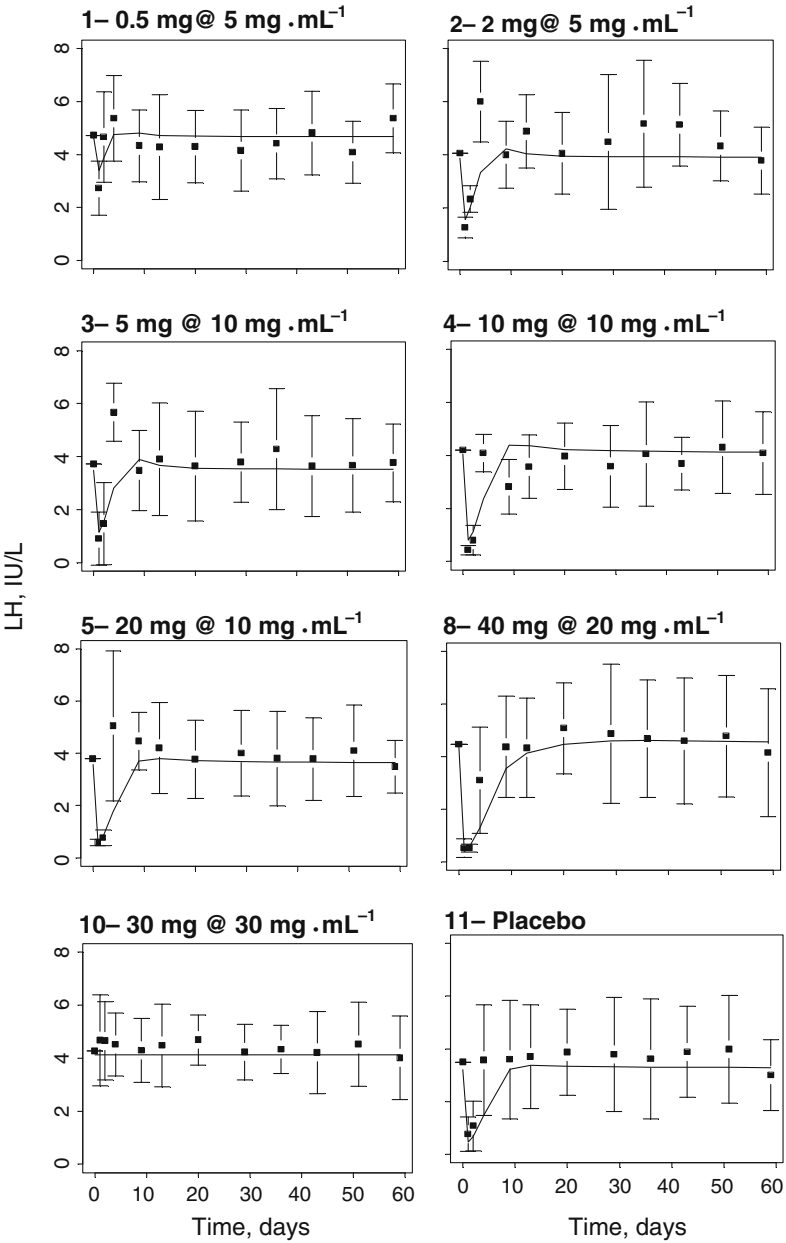

Fig. 9. The time course of observed mean (symbols) and simulated (solid line) LH levels from Study 3 (all groups not shown). The error bars correspond to one standard deviation.

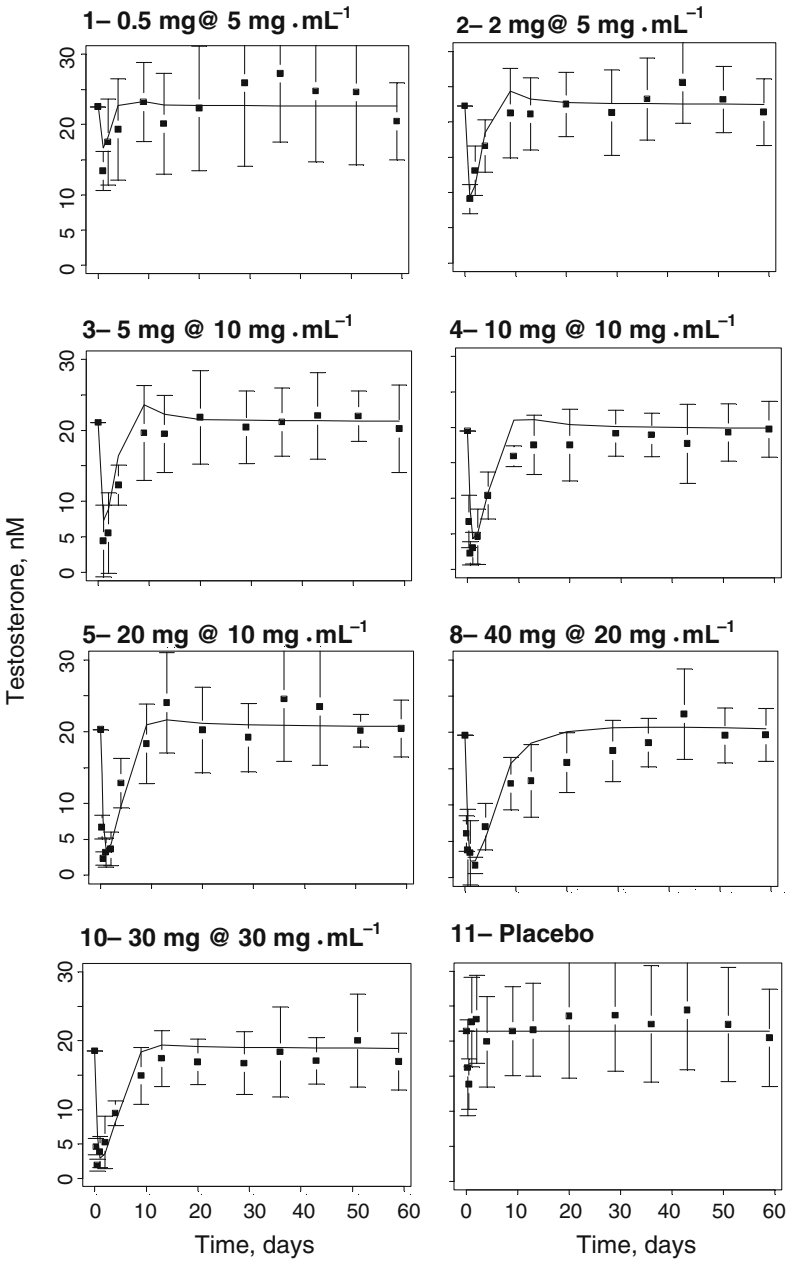

Fig. 10. The time course of observed mean (symbols) and simulated (solid line) T levels from Study 3 (all groups not shown). The error bars correspond to one standard deviation.

a pulsatile pattern to conform observed data, therefore, an empirical version of the model was employed.

The time course of LH after IV administration is well described by the proposed PD model (Fig. 5). The estimated degradation half-life of LH (2.6–3.3 hr) compares well with the literature reported values of 2–3 hr. (15, 20) The parameter $k_{deg,LH}$ was allowed to be different for groups A, D and E to account for the baseline differences. The groups exhibit slightly different baseline conditions, probably, due to highly variable nature of the input and output processes. Either the formation, degradation or both could be important determinants of the baseline differences. It is difficult to elucidate the exact contributor without additional data. Therefore, only $k_{deg,LH}$ was allowed to vary for simplicity. Other parameters were common for all the groups. A precursor dependent indirect PD response model (23, 24) was used to characterize the rebound phenomenon in LH levels (Eq. 2). The presence of LH precursor compartment (pituitary) is mechanistically well characterized (25). LH is stored in the secretory granules in a readily releasable form that is secreted via exocytosis after stimulation. The process of LH release is dependent not only on the LH levels in the pituitary but also on pulsatile GnRH levels. This interaction is modeled as a binary component assuming no basal LH release in the absence of GnRH. The choice was based on the studies involving animal models (26, 27) and a pathological condition called Kallaman's syndrome (28). According to this syndrome, lack of GnRH leads to almost complete abolition of LH. Use of a competitive interaction model (i.e. stimulatory Emax model) will not lead to complete shut-off of LH release, even when GnRH levels are zero.

The rebound phenomenon is apparent in LH time profiles for almost all the groups (Fig. 5). This pattern is not obvious for group G, most probably, due to sampling constraints. However, the presence of rebound was reported in the literature. (7, 9, 29) LH rebound was apparent after IV and SC administration of cetrorelix, a chemical analog of degarelix, in healthy volunteers (9). Similar phenomenon was also seen from the animal data after administration of degarelix, azaline or similar analogues. (7, 29)

LH was assumed to be a primary regulator of T formation (Eq. 4). This assumption is well justified as LH deprivation leads to T deficiency (30) as well as drug induced reduction of LH levels, also leads to suppression of T below the detection limit leading to chemical castration. The time course of T after IV administration is reasonably well described by the proposed PD model (Fig. 6). The estimated degradation half-life of T is 2.7 hr. The values ranging between 0.17 and 1.67 hr have been reported for this parameter (15, 20, 31). In addition to LH, there are other regulators of T secretion, supposedly, yielding a circadian rhythm to basal

T secretion (13, 32). Also, there is a long-loop and a short-loop negative feedback from T onto LH and GnRH secretion, respectively. However, such controls were not included in the model, mainly due to lack of sufficient data to estimate related parameters. Thus, the input function ($k_{f,T}$) in Eq. 12 is a complex form governed by LH levels and the factors controlling circadian rhythm. On the other hand, negligible placebo effects, relative to the drug effects, should influence neither the estimation of the PD parameters nor the choice of the dosing regimen. The IC_{50} estimate obtained from the current model was similar to the one obtained from a model that does not account for GnRH pulses (results not shown).

The presence of rebound in the T levels was not obvious due to limited data in the recovery phase. For steroid hormones like T, presence of readily releasable form (pool) is not reported. The rebound in LH levels could lead to T rebound. The estimate of IC_{50} was found to be 0.45 μg/l and it is slightly different than 0.94 μg/l (14), probably, due to different populations used in these studies, but more importantly, due to the different modeling assumptions.

Model Qualification

The model developed using Study 1 (IV) reasonably predicts the mean time course of LH and T for the Studies 2 (IV) and 3 (SC) (Figs. 7–10). There are minor discrepancies between the observed and predicted levels, possibly due to different characteristics of the patients included in the study. The subjects in Study 1 are much older (65–82 years) than those in Study 2 (19–46 years) and Study 3 (19–69 years). Nevertheless, the model predictions are in good agreement with the observed data. The model could be used to bridge two different routes of administration without having to generate additional clinical data.

Simulation of long term degarelix use, indicates that the drug effect could not be maintained as the levels of LH and T return to the baseline even if the drug concentration is maintained well above the IC_{50} estimate. (Fig. 11a) The real data after long term administration do not seem to suggest such a phenomenon (14). Clearly, the model deviates from the expectation about the long term effects. We offer the following explanation for this discrepancy. The input in the pool compartment is assumed to be unaffected by subsequent bio-processes, such as, feedback due to reduced LH or T levels. The LH levels in the pool compartment (not shown) increase monotonically when sufficient drug is present (24). With time, these amounts reach to a level where the drug fails to maintain its effect on the release from the pool compartment. Physiologically, this phenomenon of unlimited accumulation in the pool compartment is unrealistic.

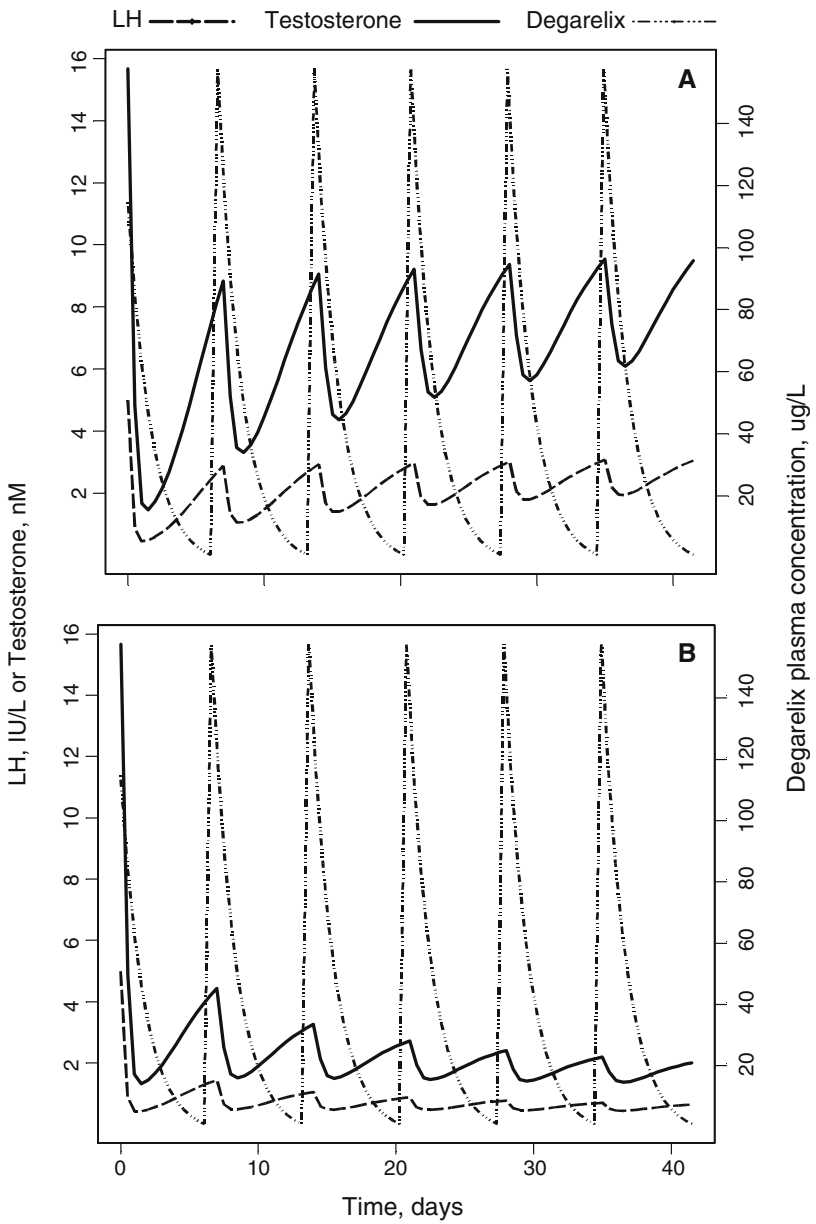

Fig. 11. Simulated time course of degarelix, LH and T after long term administration of degarelix (40 mg SC dose given once a week for 6 weeks using 20 mg/ml degarelix in the dosing solution) under (a) Final model developed based on the data (b) proposed modification to the final model (Eq. 17).

These biological molecules are in a highly regulated system and the presence of uncontrolled increase is counterintuitive to the concept of homeostasis. There are several ways to model such controls. We suggest the following modification to the model based on the physiological understanding of the HPG axis. As explained earlier, LH is stored in the secretory granules of anterior pituitary glands, which is expected to have a finite storage volume. Pituitary hormone autoregulation through intrapituitary paracrine and autocrine hormones, for example, IGF-1 for growth hormone secretion, is well documented in literature (15). These controls are important to maintain hormonal balance. Thus, we propose a feedback control on the formation of LH (Fig. 1). It can be achieved by modifying the input function of Eqs 9–17.

$$K'_{\mathrm{f,LH}} = K_{\mathrm{f,LH}} \cdot \left(1 - \frac{\mathrm{LH_{pool}} - \mathrm{LH^{ss}_{pool}}}{\Delta \mathrm{LH^{50}_{pool}} + (\mathrm{LH_{pool}} - \mathrm{LH^{ss}_{pool}})}\right) \tag{17}$$

where, $K'_{\mathrm{f,LH}}$ is the modified input rate in the $\mathrm{LH_{pool}}$ compartment, $\mathrm{LH^{ss}_{pool}}$ is the steady state $\mathrm{LH_{pool}}$ level, $\mathrm{LH^{50}_{pool}}$ is the difference in the elevated $\mathrm{LH_{pool}}$ levels and $\mathrm{LH^{ss}_{pool}}$ that decrease $\mathrm{K_{f,LH}}$ by 50%. Due to unavailability of the long term data, we could not estimate model parameters of Eq. 17. The proposed modification was conceptualized by estimates derived by eye-balling the observed data (Fig. 11b). The trough level of LH at baseline was used as a threshold, $\mathrm{LH^{ss}_{pool}} = 46.4$ IU/l, and $\mathrm{LH^{50}_{pool}} =$ 20 IU/l. The suggested modification to the model is essential for reliable prediction of long-term effects.

In conclusion, a mechanistic PKPD model explaining the interrelation between GnRH, LH, T and degarelix concentration was developed. The validity of the model accounting for the time course of drug effect and the observed rebound was justified based on the short term data. This model can be easily extended to other GnRH agonists. The PD model parameters, $k_{\mathrm{deg,LH}}$ and $k_{\mathrm{deg,T}}$, compare well with the physiological estimates, an important consideration in building mechanistic models. The model performed consistently across different routes, IV and SC, of administration. It allowed us to predict the drug effects after SC administration, while the model was developed using the IV data. We also proposed a novel modification to the precursor models that can be of general use for predicting long term responses. The reported PKPD model with the suggested modification can be used to select doses for future studies. This model can also be employed to describe the PKPD of drugs affecting HPG axis.

REFERENCES

1. T. Cook and W. P. Sheridan. Development of GnRH antagonists for prostate cancer: new approaches to treatment. *Oncologist* **5**:162–168 (2000).
2. S. L. Parker, T. Tong, S. Bolden, and P. A. Wingo. Cancer statistics, 1997. *CA Cancer J. Clin.* **47**:5–27 (1997).
3. R. S. Dutta, J. Philip, and P. Javle. Trends in prostate cancer incidence and survival in various socioeconomic classes: a population-based study. *Int. J. Urol.* **12**:644–653 (2005).
4. F. Labrie, A. Belanger, V. Luu-The, C. Labrie, J. Simard, L. Cusan, J. Gomez, and B. Candas. Gonadotropin-releasing hormone agonists in the treatment of prostate cancer. *Endocr. Rev.* **26**:361–379 (2005).
5. D. Klingmuller and H. U. Schweikert. Gonadotropin-releasing hormone: physiological and endocrinological aspects. *Recent Results Cancer Res.* **124**:1–6 (1992).
6. Plenaxis. Abarelix package insert. CDER Freedom of Information, http://www.fda.gov/cder/foi/label/2003/021320lbl.pdf. 2003. 10-4-2005.
7. P. Broqua, P. J. Riviere, P. M. Conn, J. E. Rivier, M. L. Aubert, and J. L. Junien. Pharmacological profile of a new, potent, and long-acting gonadotropin-releasing hormone antagonist: degarelix. *J Pharmacol. Exp. Ther.* **301**:95–102 (2002).
8. N. V. Nagaraja, B. Pechstein, K. Erb, C. Klipping, R. Hermann, G. Niebch, and H. Derendorf. Pharmacokinetic and pharmacodynamic modeling of cetrorelix, an LH-RH antagonist, after subcutaneous administration in healthy premenopausal women. *Clin. Pharmacol. Ther.* **68**:617–625 (2000).
9. B. Pechstein, N. V. Nagaraja, R. Hermann, P. Romeis, M. Locher, and H. Derendorf. Pharmacokinetic–pharmacodynamic modeling of testosterone and luteinizing hormone suppression by cetrorelix in healthy volunteers. *J Clin. Pharmacol.* **40**:266–274 (2000).
10. S. L. Wong, D. T. Lau, S. A. Baughman, D. Menchaca, and M. B. Garnick. Pharmacokinetics and pharmacodynamics of abarelix, a gonadotropin-releasing hormone antagonist, after subcutaneous continuous infusion in patients with prostate cancer. *Clin. Pharmacol. Ther.* **73**:304–311 (2003).
11. S. L. Wong, D. T. Lau, S. A. Baughman, N. Fotheringham, D. Menchaca, and M. B. Garnick. Pharmacokinetics and pharmacodynamics of a novel depot formulation of abarelix, a gonadotropin-releasing hormone (GnRH) antagonist, in healthy men ages 50 to 75. *J Clin. Pharmacol.* **44**:495–502 (2004).
12. C. W. Tornoe, H. Agerso, H. A. Nielsen, H. Madsen, and E. N. Jonsson. Pharmacokinetic/pharmacodynamic modelling of GnRH antagonist degarelix: a comparison of the non-linear mixed-effects programs NONMEM and NLME. *J Pharmacokinet. Pharmacodyn.* **31**:441–461 (2004).
13. K. E. Fattinger, D. Verotta, H. C. Porchet, A. Munafo, J. Y. Le Cotonnec, and L. B. Sheiner. Modeling a bivariate control system: LH and testosterone response to the GnRH antagonist antide. *Am. J. Physiol.* **271**:E775–E787 (1996).
14. C. W. Tornoe, H. Agerso, T. Senderovitz, H. A. Nielsen, H. Madsen, and E. N. Jonsson. Population PK/PD modelling of the hypothalamic–pituitary–gonadal axis following treatment with GnRH analogues. *BJCP* (2005) (submitted).
15. S. Melmed and D. L. Kleinberg. In P. R. Larsen, H. M. Kronenberg, S. Melmed, and K. S. Polonsky (eds.) *Williams Textbook of Endocrinology*, Saunders, Philadelphia (2002).
16. I. J. Clarke and J. T. Cummins. The temporal relationship between gonadotropin releasing hormone (GnRH) and luteinizing hormone (LH) secretion in ovariectomized ewes. *Endocrinology* **111**:1737–1739 (1982).
17. S. S. Yen, C. C. Tsai, F. Naftolin, G. Vandenberg, and L. Ajabor. Pulsatile patterns of gonadotropin release in subjects with and without ovarian function. *J Clin. Endocrinol. Metab* **34**:671–675 (1972).
18. M. Bergendahl, W. S. Evans, and J. D. Veldhuis. Current concepts on ultradian rhythms of luteinizing hormone secretion in the human. *Hum. Reprod. Update.* **2**:507–518 (1996).

19. R. J. Urban, W. S. Evans, A. D. Rogol, D. L. Kaiser, M. L. Johnson, and J. D. Veldhuis. Contemporary aspects of discrete peak-detection algorithms. I. The paradigm of the luteinizing hormone pulse signal in men. *Endocr. Rev.* **9**:3–37 (1988).
20. J. D. Veldhuis, J. C. King, R. J. Urban, A. D. Rogol, W. S. Evans, L. A. Kolp, and M. L. Johnson. Operating characteristics of the male hypothalamo-pituitary–gonadal axis: pulsatile release of testosterone and follicle-stimulating hormone and their temporal coupling with luteinizing hormone. *J Clin. Endocrinol. Metab*. **65**:929–941 (1987).
21. H. Agerso, W. Koechling, M. Knutsson, R. Hjortkjaer, and M. O. Karlsson. The dosing solution influence on the pharmacokinetics of degarelix, a new GnRH antagonist, after s.c. administration to beagle dogs. *Eur. J Pharm. Sci.* **20**:335–340 (2003).
22. D. M. Keenan, W. M. Sun, and J. D. Veldhuis. A stochastic biomathematical model of the male reproductive hormone system. *Siam J. Appl. Math.* **61**:934–965 (2000).
23. A. Sharma, W. F. Ebling, and W. J. Jusko. Precursor-dependent indirect pharmacodynamic response model for tolerance and rebound phenomena. *J Pharm. Sci.* **87**:1577–1584 (1998).
24. G. Movin-Osswald and M. Hammarlund-Udenaes. Prolactin release after remoxipride by an integrated pharmacokinetic–pharmacodynamic model with intra- and interindividual aspects. *J Pharmacol. Exp. Ther.* **274**:921–927 (1995).
25. J. A. Huirne and C. B. Lambalk. Gonadotropin-releasing-hormone-receptor antagonists. *Lancet* **358**:1793–1803 (2001).
26. B. M. Cattanach, C. A. Iddon, H. M. Charlton, S. A. Chiappa, and G. Fink. Gonadotrophin-releasing hormone deficiency in a mutant mouse with hypogonadism. *Nature* **269**:338–340 (1977).
27. B. D. Schanbacher, H. F. English, D. Gross, R. J. Santen, M. F. Walker, and R. E. Falvo. Animal model of isolated gonadotropin deficiency. I. Hormonal responses to LHRH immunoneutralization. *J Androl* **4**:233–239 (1983).
28. A. Iovane, C. Aumas, and N. de Roux. New insights in the genetics of isolated hypogonadotropic hypogonadism. *Eur. J. Endocrinol.* **151**(Suppl 3):U83–U88 (2004).
29. G. Jiang, J. Stalewski, R. Galyean, J. Dykert, C. Schteingart, P. Broqua, A. Aebi, M. L. Aubert, G. Semple, P. Robson, K. Akinsanya, R. Haigh, P. Riviere, J. Trojnar, J. L. Junien, and J. E. Rivier. GnRH antagonists: a new generation of long acting analogues incorporating p-ureido-phenylalanines at positions 5 and 6. *J. Med. Chem.* **44**:453–467 (2001).
30. M. Jeyakumar, R. Suresh, H. N. Krishnamurthy, and N. R. Moudgal. Changes in testicular function following specific deprivation of LH in the adult male rabbit. *J. Endocrinol.* **147**:111–120 (1995).
31. A. B. Singh, K. Norris, N. Modi, I. Sinha-Hikim, R. Shen, T. Davidson, and S. Bhasin. Pharmacokinetics of a transdermal testosterone system in men with end stage renal disease receiving maintenance hemodialysis and healthy hypogonadal men. *J. Clin. Endocrinol. Metab.* **86**:2437–2445 (2001).
32. A. Miyatake, Y. Morimoto, T. Oishi, N. Hanasaki, Y. Sugita, S. Iijima, Y. Teshima, Y. Hishikawa, and Y. Yamamura. Circadian rhythm of serum testosterone and its relation to sleep: comparison with the variation in serum luteinizing hormone, prolactin, and cortisol in normal men. *J. Clin. Endocrinol. Metab.* **51**:1365–1371 (1980).